



# Monte Carlo evaluation of particle interactions within the patient-dependent part of Elekta 6 MV photon beam applying IAEA phase space data

Deae-eddine Krim<sup>1</sup>, Dikra Bakari<sup>2</sup>, Mustapha Zerfaoui<sup>3</sup>, Abdeslem Rrhiaoui<sup>3</sup>, Yassine Oulhouq<sup>3</sup>

<sup>1</sup>Faculte des Sciences, Universite Mohammed Premier Oujda, Oujda, Morocco

<sup>2</sup>National School of Applied Sciences, University Mohamed 1st, Oujda, Morocco

<sup>3</sup>Faculty of Sciences, University Mohamed 1st, LPMR, Oujda, Morocco

## ABSTRACT

**Background:** This work aims to provide a simulated method to be used by designers of medical accelerators and in clinical centers to manage and minimize particles' interaction in the patient-dependent part of a 6 MV X-Ray Beam generated by the Elekta linear accelerator system, based on the latest GATE software version 9.0 Monte Carlo simulation, IAEA phase space data, and the last version of "Slurm" computing cluster.

**Materials and methods:** The experimental results are obtained using the Elekta 6 MV accelerator. The simulation MC developed includes the majority of the patient-dependent segments, such as Multi-Leaf Collimator (MLC), Tongue and Groove T&G, Rounded leaf Part, including the Jaws (XY). This model is used, with a simulated Iba Blue Phantom 2 homogeneous water phantom with dimensions  $480 \times 480 \times 410 \text{ mm}^3$ , positioned at a Source-to-Surface-Distance (SSD) of 100 cm, all of the interactions of the mega voltage 6 MV radiations in water are simulated. The IAEA phase space (PS) provided by the International Atomic Energy Agency database and cluster computing (Slurm HPC-MARWAN, CNRST, Morocco) are employed to reduce our simulation time.

**Results:** The results confirm that there are many interactions in all areas and the patient-dependent part's internal structures. Thus, electrons and positrons participation appear in the generated field previously designed to be an X-ray beam. Besides, to validate our implementation geometry, the PDD's and transverse profiles, at a depth ranging from 1.5 to 20 cm, for a field size of  $10 \times 10 \text{ cm}^2$ , the beam quality such as  $D_{10\%}$ ,  $d_{max}$  (cm),  $d_{80}$  (cm),  $TPR_{(20/10)}$ , the two relative differences in dose were derived on  $\sigma_i$  and  $\sigma_{i,max}$  are calculated, respectively. Additionally, gamma index formalism for 2%/2 mm criteria is used. Once and for all, we typically take a good agreement between simulation MC GATE 9.0 and the experiment data with an error less than 2%/2 mm.

**Conclusions:** In the field of X-ray photons, a significant contribution of electrons and positrons has been found. This contribution could be enough to be essential or affect the delivered dose. A good agreement of 98% between this new approach of simulation MC GATE 9.0 software based on IAEA phase space and experimental dose distributions is observed regarding the validation tests used in this task.

**Key words:** radiotherapy; Elekta linac; Monte Carlo' IAEA phase-space; GATE 9.0

*Rep Pract Oncol Radiother* 2021;26(6):928–938

**Address for correspondence:** Deae-eddine Krim, Universite Mohammed Premier Oujda Faculte des Sciences, UMP, 60000 Oujda, Morocco; e-mail: d.krim@ump.ac.ma

This article is available in open access under Creative Common Attribution-Non-Commercial-No Derivatives 4.0 International (CC BY-NC-ND 4.0) license, allowing to download articles and share them with others as long as they credit the authors and the publisher, but without permission to change them in any way or use them commercially

## Introduction

The Monte Carlo (MC) approach is included amongst the most impressive and conventional techniques. It is intensively used to simulate particles' interaction and transport in various fields. In our case, it is proven that this approach can determine the dose in complex volumes precisely, especially after the development of variance reduction techniques [1] (VRTs), which allow achieving an acceptable accuracy in the simulations, even in geometries as complex as realistic tumor shapes. This enormous progress made over the last ten years in radiotherapy has been achieved mainly by developing particles acceleration techniques and information technologies.

### Information technologies and MC codes

The MC simulation method is a class of algorithms considered to be the most powerful tool for studying the transport of ionizing radiation in radiotherapy [2]. Over the last fifty years, Monte Carlo methods have been widely applied by the scientific community. Scopus references more than [3] 7000 documents related to dosimetry and MC. GATE encapsulates the GEANT4 libraries to achieve a modular scripted MC-based simulation toolkit adapted to the field of radiation physics to be used in nuclear medicine and radiotherapy. In particular, GATE provides the capability for time-dependent modeling phenomena such as detector or source movements. Thus, it allows the simulation of time curves under realistic acquisition conditions. In this investigation, the physics list G4em-standard\_opt3 is used. The physics list G4em-standard\_opt3 uses the G4Photoelectric, G4ComptonScattering, G4GammaConversion, and G4RayleighScattering multiple scattering for all photon particles. For electrons and positrons with energy ranging from 0 to 6 MeV, G4eMultipleScattering, G4eIonisation and G4eBremsstrahlung models are used. In radiotherapy, the calculations must be exact, which is a time-consuming calculation process. Such calculation is prohibitive for routine clinical use. There have been significant developments in computer technology (use of clusters), nevertheless, multi-processors and multithreading have been used to improve software efficiency and significantly reduce computing time [4].

### Acceleration systems

The X-rays of a 4–25 MV energy range produced by medical linear accelerators are universal photons' beams used to treat tumors that occur at a depth below the skin surface. Fundamental requirements for radiation therapy improvements include characterizing the radiation beam for various delivery techniques and treatment planning and delivery schedules [5, 6]. To reach this target, it is necessary to understand the radiation transport in the linac head and the influence on the beam incident on the patient.

Several researchers have applied Monte Carlo techniques to study the distribution of radiation therapy treatment planning for photon and electron beams inside the patient with acceptable results. However, the interactions that happened precisely in the linac head and, especially, in the patient-dependent part remain unknown. This part contains all moving components, such as the secondary collimator's jaws and the multi-leaf collimator (MLC). The moving of those components can create an undesirable effect on the field.

Accordingly, this paper is organized as follows; the patient-dependent part of the Elekta platform accelerator is modeled, in which all steps used in our simulation strategy are fully described. Moreover, in the third section, the results obtained discuss each component's influence on Elekta 6 MV linac photon beams. Besides, a comparison of simulated and experiment PDD's and dose profiles' distributions using the SLURM-cluster has been established and conclusions have been drawn in the fourth section.

## Materials and methods

The Software and the Hardware requirements used for this study were as follows:

### Hardware fundamentals

The energy photon beam (X-6 MV) was used in this study, with a reference dose rate of 400 MU/min, delivered by the ELEKTA platform. Furthermore, dosimetry calculation was carried out according to AAPM's TG-51 protocol [7]. The experiment data were obtained using a cylindrical ionization chamber, type 9732-2 with an active volume of 0.125 cm<sup>3</sup>, mounted over a motorized

guide in a resistance temperature detector 3D water phantom at an SSD = 100 cm.

### Software requirements

To accomplish this simulation, GATE version 9.0 [8] (Feb. 2020) was applied in Ubuntu LTS 19. To store and analyze output and input data through simulation, ROOT object-oriented software version 6.14 was applied [9]. To visualize and check the geometry of the component, graphical interfaces, which were utilized as flow: running GATE in QT mode [10] (GEANT4 QT User Interface).

### Particle interactions simulation

The exact simulation of any system requires the simulation of all physical particles (events) inside the logical world volume, which takes place in the real world. Considering our simulation, the primary and secondary particles created inside the linac system present the range of megavoltage energy. Hence, the standard model of electromagnetic interactions and that of electromagnetic standard type opt3 are used [8].

### Implementation of Elekta linac geometry

Relying on detailed information cited in the usually published advanced papers, head linac has been simulated using GATE [11]. Figure 1 displays the global variant structure of the technique applied to simulate the linear accelerator and the water phantom considered in this study.

Simulation components shown in Figure 1 can be summed up in four steps, as in Table 1:

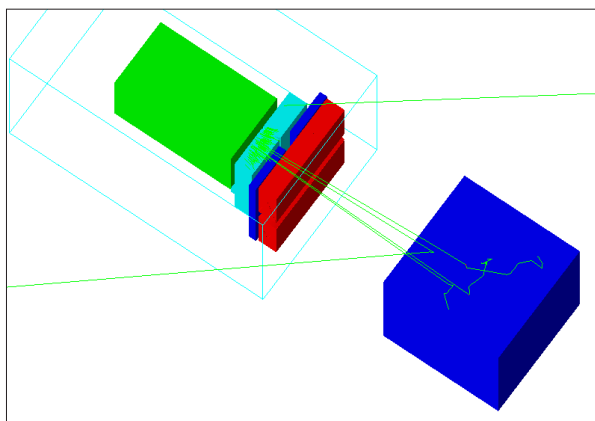


**Figure 1.** The composition of the system geometry employed in the simulation of linac, using GATE 9.0

**Table 1.** The structural configuration of linac modeling converted on MC GATE software

Linac component	Converted structure GATE 9.0 version	
X-ray target	-----	-----
Primary collimator	-----	-----
Flattening filter	IAEA Ph. Sp	Insert Box
Transmission chambers	-----	-----
Mylar mirror	-----	-----
Multi-leaf Collimator	Insert Trapezoid Box, part of Circle	
Asymmetric jaws X and Y	Insert Trapezoid Box, part of Circle	
Phantom	Insert Box	

- phase space IAEA — the IAEA phase space stores millions of particles by the simulation of the independent patient part I.P.P. with all components based on the vendor’s detailed information and by the use of the EGSnrc version V4-r2-3-0. Furthermore, the advantage is that the I.P.P components (including the X-ray target, primary collimator, flattening filter F.F, transmission chamber, backscatter plate, and finally the mylar mirror) have never been seen changed during a real treatment. Therefore, the IAEA phase space presents a perfect approach to minimize the time of calculation;
- multi-leaf collimator (MLC) — made of tungsten alloy, about 1 and 7.7 cm of thickness and height, respectively, located just below the Phase Space position (28 cm), used for precise treatment and most accurate conformal beam shaping for treatments;
- secondary collimators (X, Y) are made of tungsten alloy about 10 cm of thickness used to minimize the inter-leaf leakage and set the treatment field’s overall size;
- phantom — box of water with sizes 480 x 480 x 410 mm<sup>3</sup> similar to the Iba blue water phantom located at a source surface distance of 100 cm from the target.

### Simulation techniques

Simulation techniques can be summed up in two steps.

Phase spaces implementation (Fig. 1):

- defining the first phase-space plan, located below the IAEA phase space, is to study the distribution

of the IAEA phase space particles before all interactions with the variant part of the linac system;

- the second phase-space located below the MLC is employed to show the distribution of leakage particles passing through the MLC;
- the third phase-space is located in SSD = 100 cm to evaluate the geometry of the variant part of the linear accelerator.

Actors:

- the track length and the secondary production actors used in all parts of the logical world volume;
- the number of particles entering volume actor used inside each component (MLC and jaws).

Actors are tools that allow users to interact with the code GATE; they can collect information during the simulation. Furthermore, to extract the distribution of dosimetric parameters and accelerate the simulation process “to reduce the CPU time”, the Actors used in this task are DoseTool and KillTool, respectively.

Figure 2 shows exactly the approach used by the algorithm DoseTool integrated into GATE to calculate the Percentage Depth Dose (PDD) and the horizontal dose profiles’ distributions with sizes of voxels  $2 \times 5 \times 5$ ,  $5 \times 2 \times 5$ .mm<sup>3</sup> and  $5 \times 5 \times 2$ .mm<sup>3</sup>, respectively.

The cluster computing technique (SLURM-CNRST Team Morocco) was utilized. Openmosix cluster platform used to split the main GATE code to 1000 sub-main codes into 100 jobs,

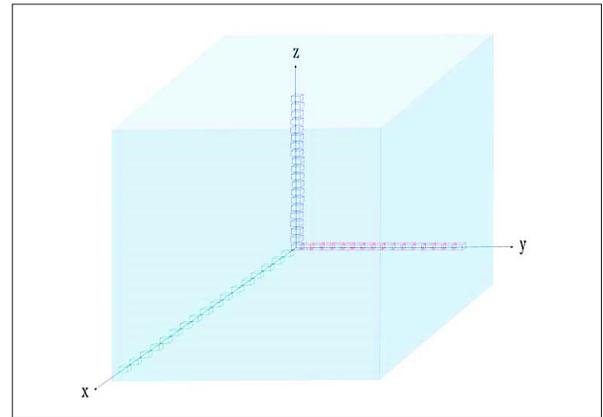


**Figure 2.** Schematic view of doses used in-depth and lateral dose profiles curve calculations

as presented in Figure 3 (100 nodes in parallel: 15 CPUs, two threads per core). During the simulation MC, the parallelized simulations’ ROOT files output will be merged to provide a single output file.

### Validation tests

Many tests are performed to validate simulation against measurement data. Each one has advantages and restrictions, but as a whole, they present the best standard and the most well-known tests in dose computation. The results obtained compared to the experimental data using the parameter  $\sigma_i$  allowing to construct the mean, standard error between each point measured experimentally and that calculated by GATE, with the equation:

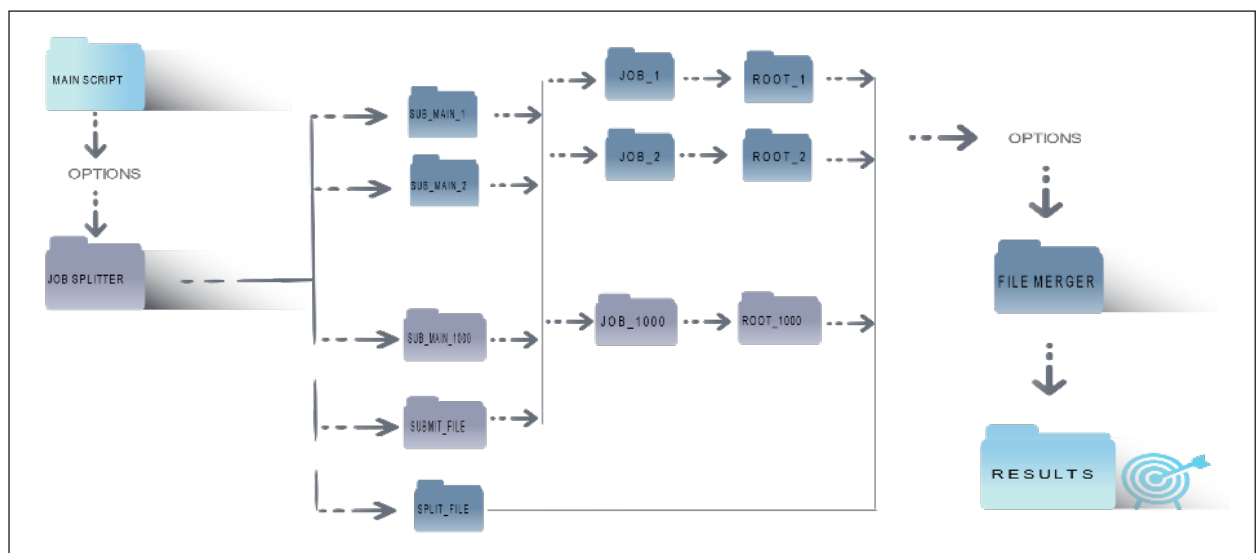


**Figure 3.** Schematic overview of the splitting and merging approach using Openmosix cluster platform

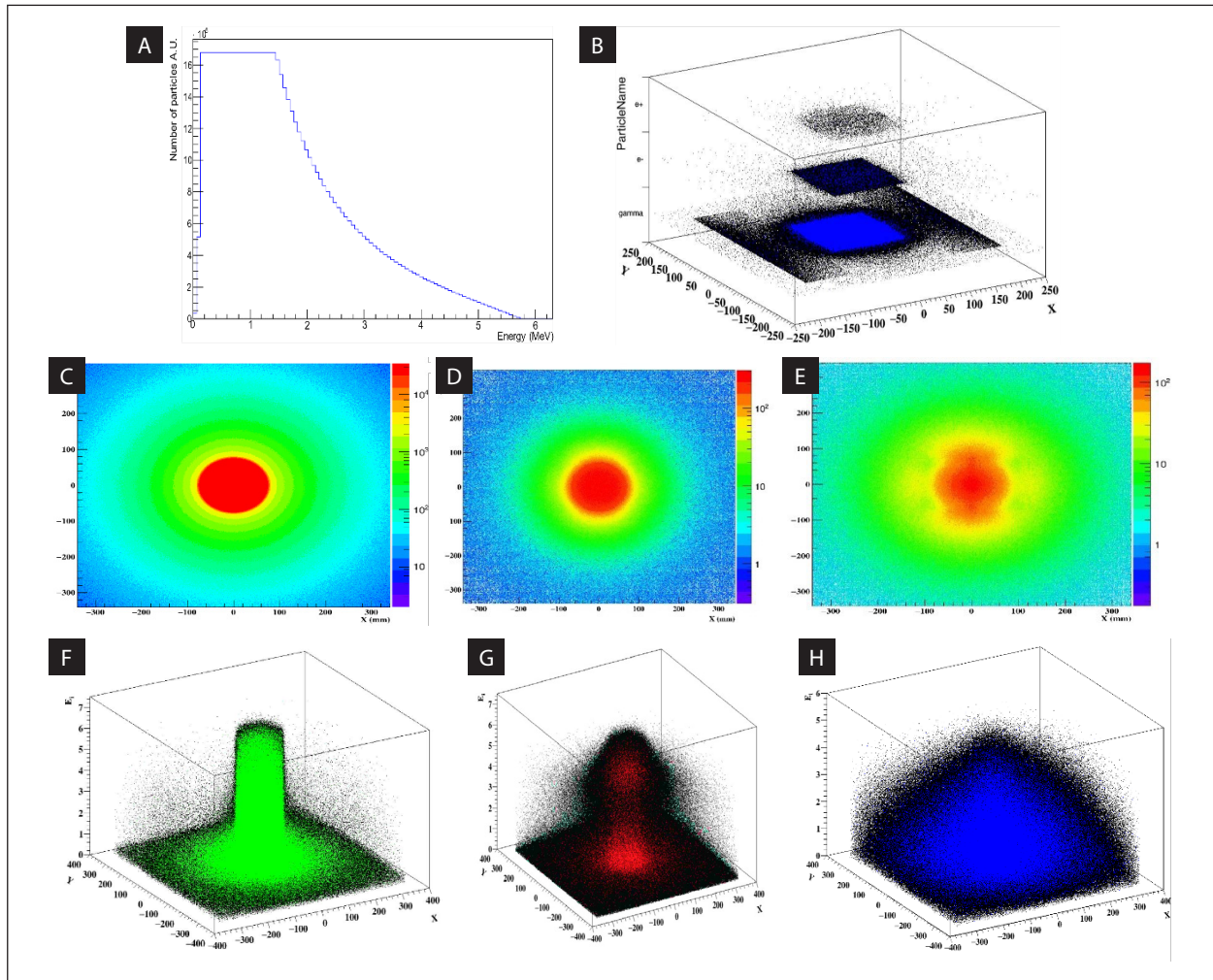


**Figure 4.** Correlation between the ideal coordinates of IAEA PS and the new coordinate defined in this task. **A.** Energy spectrum (average energy 1.315 MeV); **B.** Distribution of each name of particle versus (X, Y). **C–E.** X versus Y of photons, electrons and positrons, respectively. **F–H.** Energy versus X and Y of photons, electrons and positrons, respectively

$$\sigma_i = \frac{1}{n} \sum_i^n \frac{|(D_{S_i} - D_{S_{refi}})|}{D_{refi}} \quad (1)$$

In the low dose, the use of  $\sigma_i$  error could lead to high overall errors. Furthermore, in the case of lateral profiles, the agreement procedure with measurements was roughly calculated by:

$$\sigma_{i,max} = \frac{1}{n} \sum_i^n \frac{|(D_{S_i} - D_{S_{refi}})|}{D_{S_{refi,max}}} \quad (2)$$

Where the  $| (D_{S_i} - D_{S_{refi}}) |$  describes the difference of the dose among the points measured and calculated. Nevertheless,  $D_{S_{refi,max}}$  represents the dose of maximal experimentally measured.

Extensive comparisons among the simulation and experiment dose distributions for photon beam Elekta linac are completed by implementing  $\gamma$  index analysis following the formalism suggested in [12–14].

The proportion among doses measured and calculated with the GATE utilized as a second test. This parameter was defined for each measurement point  $dp_m$  by:

$$R_i = \frac{D_{S_c}(i)}{D_{S_m}(i)} \quad (3)$$

Where  $D_{S_c}$  and  $D_{S_m}$  represent, respectively, the calculated and the measured doses, for each point (i) inside the distribution related to distance.

## Results and discussion

### Analysis of the IAEA phase space

The IAEA phase space stores millions of particles. The classical convention of this file represents each particle position by its Cartesian coordinates ( $x, y, z$ ), the direction by ( $u, v, w$ ), the particle energy, and each type of particle's weight. Besides, to study all particles' distributions inside this file, correlations between the ideal coordinates and the new ones available in the phase space plan actor must be thought of (see Fig. 4).

### Phase space of leakage particles from MLC to jaws (X, Y)

The actor could create a map of the number of particles produced out of its volume and interacting within. Then, the particle is recorded once in each voxel where it interacts [8].

The results of this phase space plan and the number of particles entering volume MLC, using the T&G and rounded part in the MLC shape are presented in Figure 5.

As highlighted, the use of T&G minimizes the transmission of particles between leaves. However, the rounded part of leaves increases the leaf end leakage; this part presents the vertical part of the field (see Fig. 5AB).

Moving to the actor (number of particles entering volume) and according to Figure 5CD, more photons produce new interactions compared to electrons and positrons. Besides, the number of electrons and positrons decreases rapidly as the depth (MLC area) increases. However, the number of photons decreases slightly in the MLC area as the depth increases. As a result, many photons are observed in the central axis and their number decreases going away from the center.

### Track length and secondary production

The parameter most used in GATE to calculate the free path of particles before interacting is the track length actor Figure 6 [8].

According to Figure 6, the number of photons with track lengths between 26 and 60 mm is more

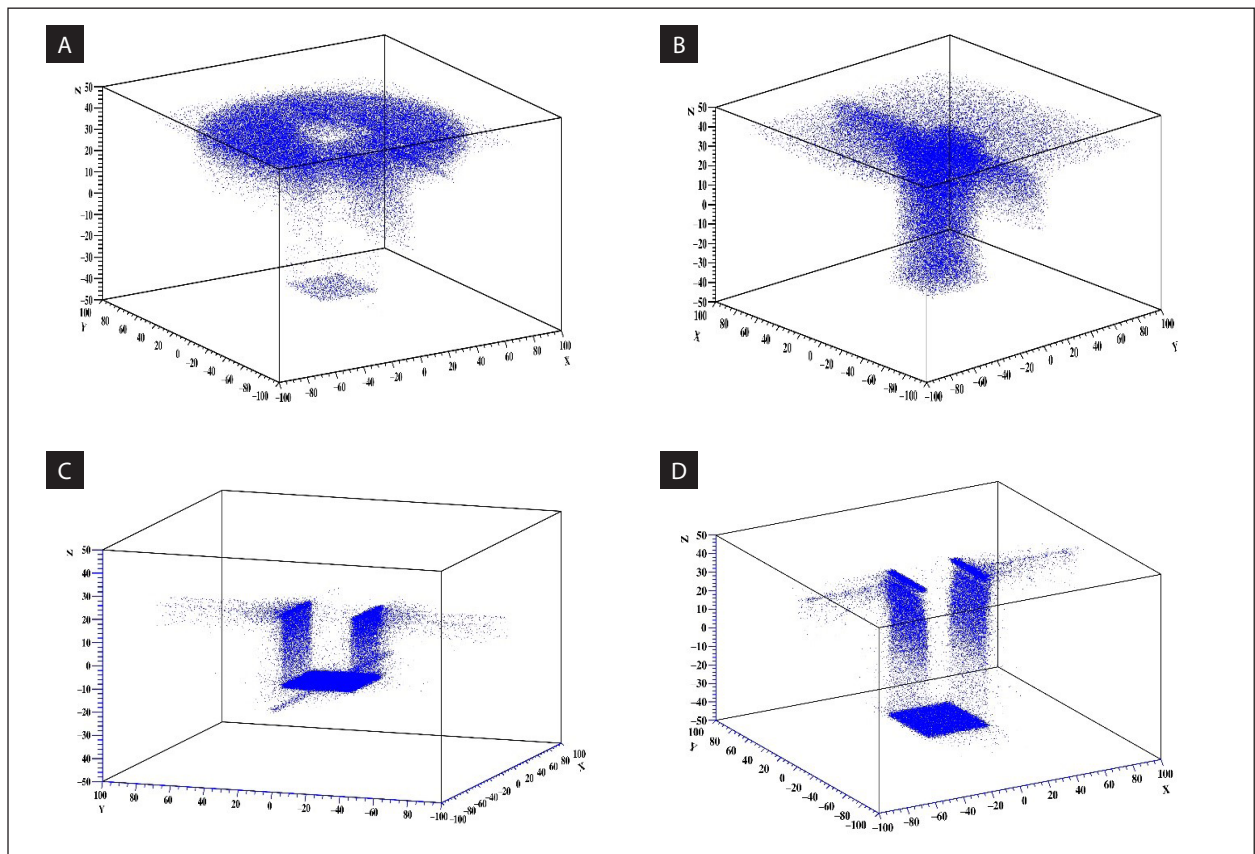


**Figure 5.** Distribution of leakage particles presented by photons and electrons versus (X, Y, Z) axis inside the MLC volume, (A) and (B), respectively. C and D show gamma and electron interaction inside the Jaws X and Y volumes

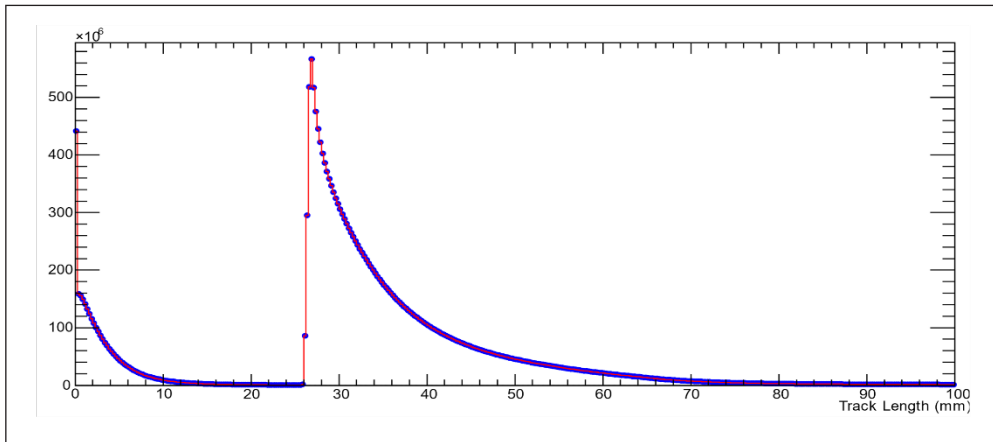


Figure 6. The track length associated to photon simulation

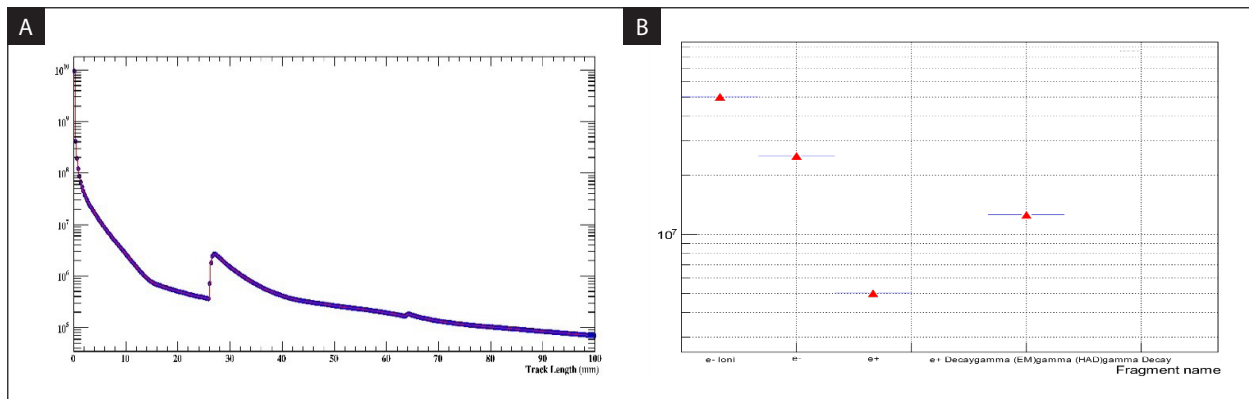


Figure 7. A. Electrons and positrons track length actor. B. Name of fragment positions

significant than that whose track length is between 0 and 10 mm. Thus, the first amount of photon presents the photons interacting with the rounded part of MLC and Jaws. In comparison, the second number of photons with a track length between 0 and 10 mm presents photons interacting with the MCL area.

Electrons and positrons constitute the charged particles of this simulation. According to Figure 7A, most of these particles' track length is between 0 and 10 mm (0–1 mm for positrons). Nevertheless, a small number of electrons is observed to have track lengths between 26 and 36 mm. As a result, and according to Figure 7B, the electrons represent the absolute majority of secondary production within the patient-dependent linac head part.

### Dose calculation validation and efficiency

To adequately validate the photon beam's quality taken by the simulation GATE against the accurate

measured data and according to international recommendations (IAEA TRS398) [15, 16], the index of quality tissue phantom ratio (TPR) in water for the square field  $10 \times 10 \text{ cm}^2$  the  $D_{10}(\%)$ ,  $d_{max}(cm)$  and  $d_{80}(cm)$  are reported and compared as shown in Table 2.

According to Table 2, deviation among measurement and GATE data for the relative dose at a depth of 10 cm was discovered to be less than 1.4 % by computation. Moreover, the highest variance associated with the dose's depth was less than 3 mm, and the variation associated with it was less than 1.1%. To sum up the dissimilarity observed at this comparison among GATE computations and measurements is down up to 2 %.

Transferring immediately to examine the produced results with more powerful tests, the simulated and experimental PDD is plotted in Figure 8 for a 6 MeV photon beam Elekta and a fixed field dimension  $10 \times 10 \text{ cm}^2$ . All curves (measured and cal-

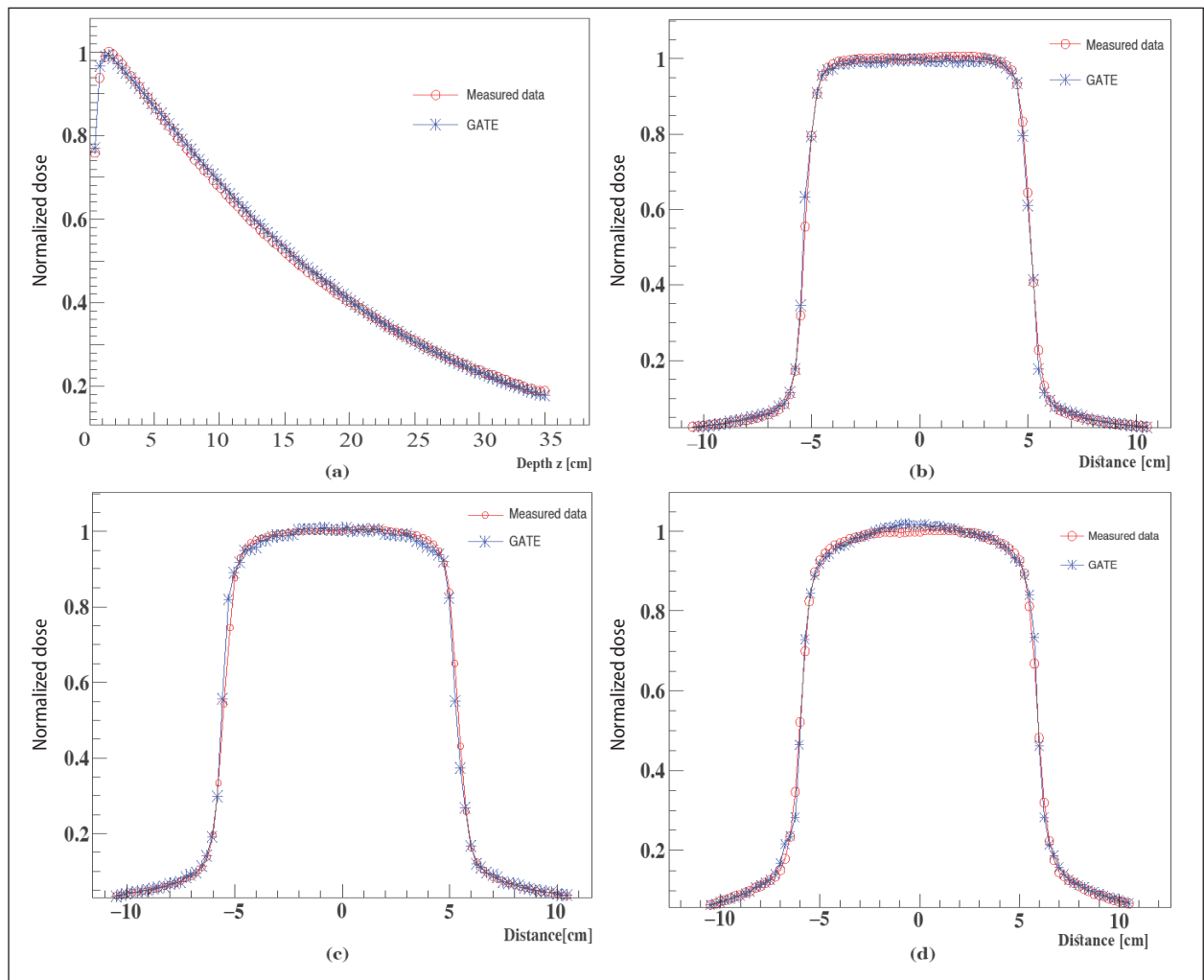
**Table 2.** Comparison of calculated and measured beam quality parameters

Parameters	GATE simulation	Measured data	Error estimation
$D_{10}$ (%)	0.68411	0.6741	1.4 %
$d_{max}$ [cm]	1.417	1.5	$0.83 < 3$ mm
$d_{90}$ [cm]	6.8	6.5	3 mm
$TPR_{(20/10)}$	0.682345	0.68846	$6.115 \times 10^{-3}\%$

culated by GATE) are normalized to the maximum dose  $d_{max}$  (cm) and compared through the usage of  $\sigma_1$  and  $\sigma_{1,max}$  parameters Figure 9. Furthermore, the frequency of the ratio and the gamma index histograms of dose differences are shown in Figure 10.

According to Figure 8, it can be concluded that the approach exploited in this Monte Carlo simulation model is very compatible with the measured data. It can be observed that the curve of the GATE MC simulation (blue curve) is confused with the experiment data (red curve).

Figure 9A shows a recording of a high overestimation in the build-up region (earlier than the maximum ionization dose), with dose divergences near to 3% compared to all the rest of interval depth  $z$  (mm). Furthermore, these overestimates between the experimental and simulated output are from the impact of the active ionization chamber volume size in which a large dose gradient occurs.

**Figure 8.** Comparison of simulated and experimental measured PDD and transversal profile at a depth of 1.5, 10, and 20 cm for 6 MeV photon beam for field sizes  $10 \times 10$  cm<sup>2</sup>

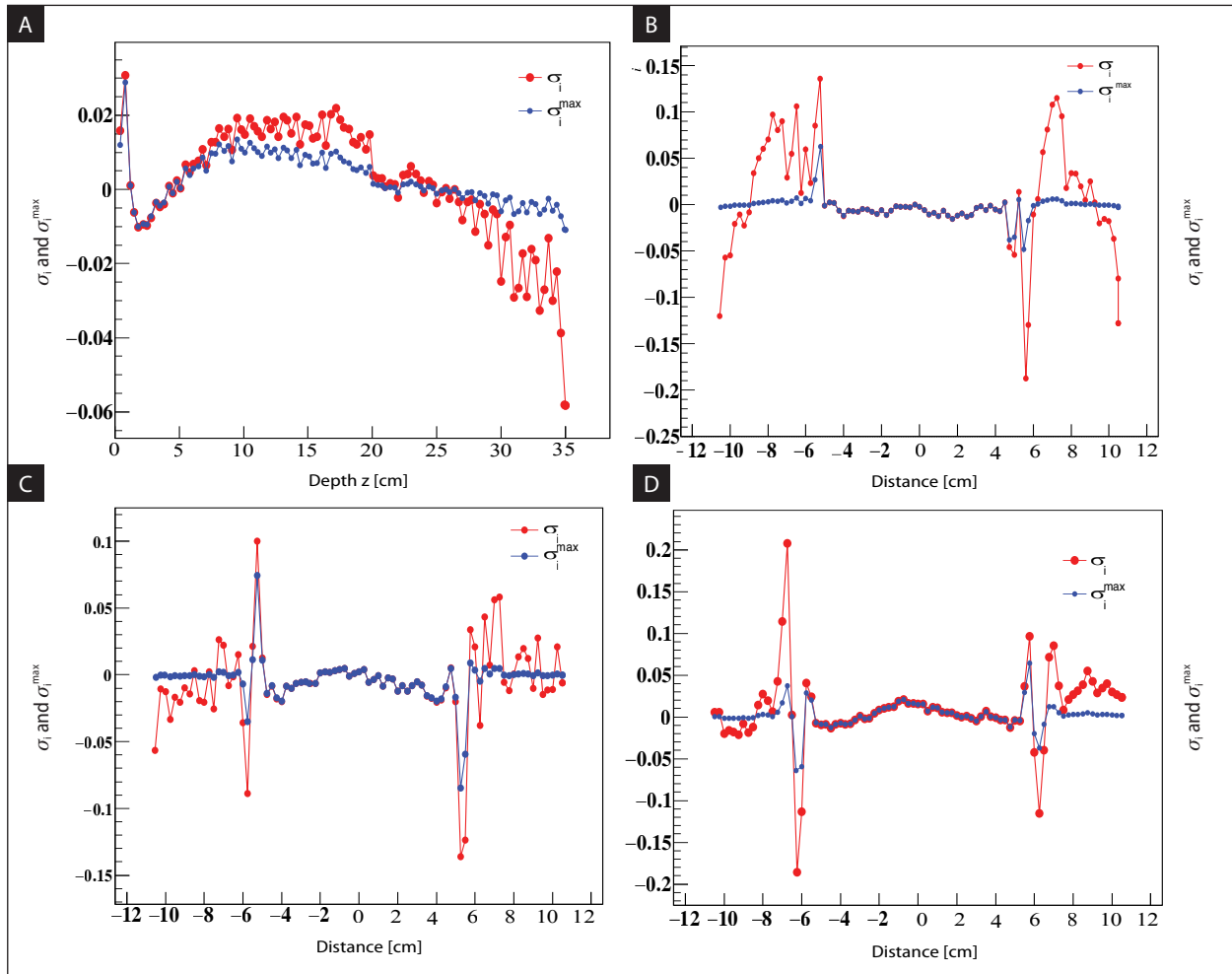


**Figure 9.** Comparison of PDD and transversal profile at a depth of 1.5, 10, and 20 cm using  $\sigma_I$  and  $\sigma_{I,max}$

Otherwise, Figure 9B–D, show the evaluation of dose differences with  $\sigma_I$  indicate that experimental and simulated curves vary in more than  $-1\%$  in depth between 30 and 35 cm. This big diffusion demonstrated the law cited in the validation test section, that  $\sigma_I$  has a limitation in the evaluation of low dose errors compared to  $\sigma_{I,max}$  that range in the interval between  $-1\%$  and  $1\%$  in low dose interval.

Relating to Figure 10B, the histogram of statistics based on  $R_I$  parameter about the differences for the PDD curves is close to a Gaussian distribution (the curve red taken by a Gaussian fit function) has been observed. However, these results indicate the systematic dissimilarities around unit “1”.

Figure 8B–D show lateral dose profiles at 1.5, 10 also 20 cm in depth. The evaluation of dose differences parameters  $\sigma_I$  and  $\sigma_{I,max}$  show that experimental and simulated curves differ in no more than 3% for the  $\sigma_{I,max}$  parameter. But, in the case of the

use of  $\sigma_I$  parameter, the differences were extremely increased, to about 15%. Whereas, the dissimilarity inside the interval from  $-5$  cm to  $5$  cm which represents the important part of the profile is closed to 2%. Furthermore, Figure 10 (a) displays the gamma index’s distributions and the ratio frequency fitted for PDD, profiles at depths 1.5, 10, and 20 cm, respectively. According to the results, the distribution of the gamma index shows a mean less than 1. It confirms that more than 98% of points pass the gamma index criteria.

The most significant dissimilarities drawn from Figure 8 to 10 between experimental and simulated doses are at the penumbra area and build-up regions. Moreover, the increase of differences by influencing the size of the active ionization chamber volume in the area in which a large dose gradient occurs has been proved. In this case, the ionizing chamber measurement was strongly averaged.

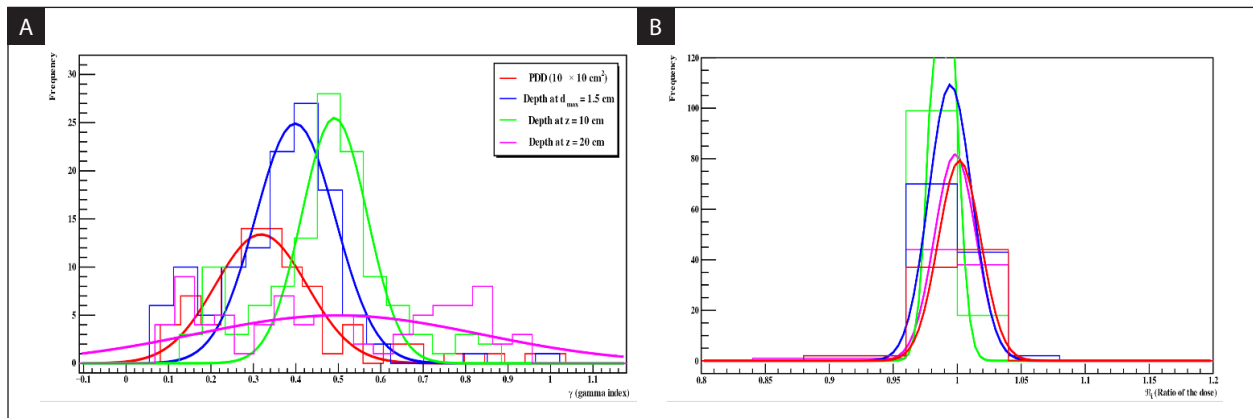


**Figure 10.** Comparison of PDD and transversal profile at a depth of 1.5, 10, and 20 cm using Frequency of the Ratio  $R$ , and  $\gamma_{index}$  2%/2mm criteria distributions

## Conclusion

The interactions of different particles with the various components of the accelerator in the patient-dependent part were studied to improve dose accuracy. GATE 9.0 software and calculation grid (Slurm cluster) are exploited. The phase space technique was used allowing to extract the energy spectrum of all particles from the IAEA phase space. In the field of X-ray photons, a significant contribution of electrons and positrons has been found. This contribution could be enough to be essential or affect the delivered dose. This change is due to the particles produced by primary photons' interaction with the accelerator (independent part, MLC, and Jaws). Compared to the experiment data, the quality of the achieved results for the investigated parameters confirms the accuracy of the proposed model based on IAEA phase space data. A good agreement of 98% between simulation MC GATE 9.0 software applying IAEA phase space data and experimental dose distributions is observed regarding the validation tests used in this task. Likewise, these results are harmonious with the theoretical value based on Virtual Source Model mentioned by Grevillot [17], and Arif [18].

## Conflict of interest

None declared.

## Funding

None declared.

## Acknowledgments

This project is supported by the National Center for Scientific and Technical Research CNRST (HPC-Marwan cluster). The authors would like to acknowledge the open-GATE collaboration for implementing the toolkit.

## References

- Zheng Yu, Qiu Y, Lu P, et al. An improved on-the-fly global variance reduction technique by automatically updating weight window values for Monte Carlo shielding calculation. *Fusion Engineer Design*. 2019; 147: 111238, doi: [10.1016/j.fusengdes.2019.06.011](https://doi.org/10.1016/j.fusengdes.2019.06.011).
- Junior JPR, Salmon H, Menezes AF, et al. Simulation of Siemens ONCOR™ Expression linear accelerator using phase space in the MCNPX code. *Progress in Nuclear Energy*. 2014; 70: 64–70, doi: [10.1016/j.pnucene.2013.07.013](https://doi.org/10.1016/j.pnucene.2013.07.013).
- Papadimitroulas P. Dosimetry applications in GATE Monte Carlo toolkit. *Phys Med*. 2017; 41: 136–140, doi: [10.1016/j.ejmp.2017.02.005](https://doi.org/10.1016/j.ejmp.2017.02.005), indexed in Pubmed: [28236558](https://pubmed.ncbi.nlm.nih.gov/28236558/).
- Gardner M, McNabb A, Seppi K. A speculative approach to parallelization in particle swarm optimization. *Swarm Intellig*. 2011; 6(2): 77–116, doi: [10.1007/s11721-011-0066-8](https://doi.org/10.1007/s11721-011-0066-8).
- Ahnesjö A, Aspradakis MM. Dose calculations for external photon beams in radiotherapy. *Phys Med Biol*. 1999; 44(11): R99–155, doi: [10.1088/0031-9155/44/11/201](https://doi.org/10.1088/0031-9155/44/11/201), indexed in Pubmed: [10588277](https://pubmed.ncbi.nlm.nih.gov/10588277/).
- Jenkins TM, and Ro. *Monte Carlo Transport of Electron and Photons*. Plenum, New York 1988: 453–468.
- Almond PR, Biggs PJ, Coursey BM, et al. AAPM's TG-51 protocol for clinical reference dosimetry of high-energy photon and electron beams. *Med Phys*. 1999; 26(9): 1847–1870, doi: [10.1118/1.598691](https://doi.org/10.1118/1.598691), indexed in Pubmed: [10505874](https://pubmed.ncbi.nlm.nih.gov/10505874/).
- Jan S, Santin G, Strul D. GATE: a simulation toolkit for PET and SPECT. *Phys Med Biol*. 2004; 49(19): 4543–4561, doi: [10.1088/0031-9155/49/19/007](https://doi.org/10.1088/0031-9155/49/19/007), indexed in Pubmed: [15552416](https://pubmed.ncbi.nlm.nih.gov/15552416/).

9. Antcheva I, Ballintijn M, Bellenot B, et al. ROOT — A C++ framework for petabyte data storage, statistical analysis and visualization. *Comp Phys Communicat.* 2011; 182(6): 1384–1385, doi: [10.1016/j.cpc.2011.02.008](https://doi.org/10.1016/j.cpc.2011.02.008).
10. Agostinelli S, Allisonas J, Amako K. Geant4 — a simulation toolkit. *Nucl Instrum Methods Phys Res Sect A.* 2003; 506(3): 250–303, doi: [https://doi.org/10.1016/S0168-9002\(03\)01368-8](https://doi.org/10.1016/S0168-9002(03)01368-8).
11. Li J, Zhang XZ, Gui LG, et al. Clinical Feasibility of Leakage and Transmission Radiation Dosimetry Using Multileaf Collimator of ELEKTA Synergy-S Accelerator During Conventional Radiotherapy. *Journal of Medical Imaging and Health Informatics.* 2016; 6(2): 409–415, doi: [10.1166/jmihi.2016.1706](https://doi.org/10.1166/jmihi.2016.1706).
12. Low DA, Dempsey JF. Evaluation of the gamma dose distribution comparison method. *Med Phys.* 2003; 30(9): 2455–2464, doi: [10.1118/1.1598711](https://doi.org/10.1118/1.1598711), indexed in Pubmed: [14528967](https://pubmed.ncbi.nlm.nih.gov/14528967/).
13. Van Dyk J, Barnett RB, Cygler JE, et al. Commissioning and quality assurance of treatment planning computers. *Int J Radiat Oncol Biol Phys.* 1993; 26(2): 261–273, doi: [10.1016/0360-3016\(93\)90206-b](https://doi.org/10.1016/0360-3016(93)90206-b), indexed in Pubmed: [8491684](https://pubmed.ncbi.nlm.nih.gov/8491684/).
14. Low DA, Harms WB, Mutic S, et al. A technique for the quantitative evaluation of dose distributions. *Med Phys.* 1998; 25(5): 656–661, doi: [10.1118/1.598248](https://doi.org/10.1118/1.598248), indexed in Pubmed: [9608475](https://pubmed.ncbi.nlm.nih.gov/9608475/).
15. Teixeira MS, Batista D, Braz D, et al. Monte Carlo simulation of Novalis Classic 6 MV accelerator using phase space generation in GATE/Geant4 code. *Progr Nucl Energy.* 2019; 110: 142–147, doi: [10.1016/j.pnucene.2018.09.004](https://doi.org/10.1016/j.pnucene.2018.09.004).
16. Tuğrul T, Eroğul O. Determination of initial electron parameters by means of Monte Carlo simulations for the Siemens Artiste Linac 6 MV photon beam. *Rep Pract Oncol Radiother.* 2019; 24(4): 331–337, doi: [10.1016/j.rpor.2019.05.002](https://doi.org/10.1016/j.rpor.2019.05.002), indexed in Pubmed: [31193931](https://pubmed.ncbi.nlm.nih.gov/31193931/).
17. Grevillot L, Frisson T, Maneval D, et al. Simulation of a 6 MV Elekta Precise Linac photon beam using GATE/GEANT4. *Phys Med Biol.* 2011; 56(4): 903–918, doi: [10.1088/0031-9155/56/4/002](https://doi.org/10.1088/0031-9155/56/4/002), indexed in Pubmed: [21248389](https://pubmed.ncbi.nlm.nih.gov/21248389/).
18. Efendi MA, Funsian A, Chittrakarn T, et al. Monte Carlo simulation using PRIMO code as a tool for checking the credibility of commissioning and quality assurance of 6 MV TrueBeam STx varian LINAC. *Rep Pract Oncol Radiother.* 2020; 25(1): 125–132, doi: [10.1016/j.rpor.2019.12.021](https://doi.org/10.1016/j.rpor.2019.12.021), indexed in Pubmed: [31920464](https://pubmed.ncbi.nlm.nih.gov/31920464/).